THE JOURNAL OF NAVIGATION (2017), **70**, 686–698.
doi:10.1017/S0373463316000825

Accounting for Inter-System Bias in DGNSS Positioning with GPS/GLONASS/BDS/Galileo

Hui Liu, Bao Shu, Longwei Xu, Chuang Qian, Rufei Zhang and Ming Zhang

(*GNSS Research Center, Wuhan University, Wuhan, China*)
(E-mail: baos613@whu.edu.cn)

Code Differential Global Positioning System (DGPS) is widely used in satellite navigation and positioning because of its simple algorithm and preferable precision. Multi-Global Navigation Satellite System (GNSS) is expected to enhance the accuracy, reliability and availability of Differential GNSS (DGNSS) positioning. Traditional DGNSS models should set separate clock parameters due to the clock differences between the different systems. Awareness of the Inter-System Bias (ISB) could help to maximise the redundancy of the positioning model, thus improving the performance of multi-GNSS positioning. This paper aims to examine the inter-system bias of GPS/GLONASS/BeiDou (BDS)/Galileo and their benefits in DGNSS positioning. Results show that Differential ISB (DISB) characteristics vary with different receiver types and systems. The size of DISB could reach metre-level and the precision of estimated DISBs can reach approximately several centimetres within tens of epochs. Therefore, a new real-time DGNSS model that accounts for ISB is proposed. After differential ISBs are initialised, positioning with four satellites from arbitrarily the same or different systems can be realised. Moreover, compared with the traditional DGNSS model, the precision of the positioning results with the new model are obviously improved, especially in harsh environments.

KEYWORDS

1. Differential positioning. 2. Multi-GNSS. 3. Inter-system bias. 4. Limited satellites visible.

Submitted: 1 February 2016. Accepted: 5 November 2016. First published online: 1 February 2017.

1. INTRODUCTION. Multi-Global Navigation Satellite System (GNSS)-combined positioning and navigation has been a trend since the steady development of new global navigation satellite systems such as Galileo and the BeiDou System (BDS). This has the potential to improve the accuracy, reliability and availability of satellite positioning, navigation and timing. Many studies (Shi et al., 2013; Deng et al., 2014; He et al., 2014) have investigated the processing of multi-GNSS data. According to these papers, the precision

and the success rate of ambiguity resolution, as well as the initialisation time, have been improved because of the increasing number of observed satellites.

However, these studies have mainly focused on loose combination (Zhang et al., 2003): one pivot satellite for each system in relative positioning and one receiver clock parameter for one system in single-point positioning. To study the interoperability of a multi-system, an Inter-System Bias (ISB) must be involved. The ISB includes the timescale difference and the receiver hardware delay difference in two signals between two systems (Cai and Gao, 2009; Dalla Torre and Caporali, 2015). The time bias is eliminated and only the receiver-specific and signal-specific hardware difference remains in the double differenced observation (Montenbruck et al., 2011). The ISB for a differential model is mainly affected by the hardware delay of GNSS receivers similar to the receiver Differential Code Bias (DCB). The DCB, expressed as the difference in hardware delay between two frequencies in one system, can reach tens of nanoseconds (Schaer, 1999). The receiver hardware delay is less affected by the temperature and other environmental factors, and thus the variation of the receiver DCB is small (Sardón and Zarraoa, 1997; Schaer, 1999). The ISB related to two receivers and two systems can also be stable (Montenbruck et al., 2011). Based on previous ISB research, a few studies (Odijk and Teunissen, 2013; Paziewski and Wielgosz, 2014; Odolinski et al., 2014) have investigated the GPS/Galileo combination in relative positioning. The size of ISBs may vary with different receivers. For differential positioning related to two receivers, the size of the Galileo-GPS code ISB can be a few hundred metres in some receiver pairs of different manufacturers (Odijk and Teunissen, 2013). One can take full advantage of the measurements by applying *a priori* corrections for the receiver-dependent differential ISBs to maximise the redundancy. The introduction of the known ISB parameter can improve the performance of the carrier phase ambiguity resolution compared with loose combinations (Paziewski and Wielgosz, 2014; Odolinski et al., 2014).

In differential positioning, code-based DGNSS is also widely used in navigation, surveying and mapping (Kremer et al., 1990; Ashkenazi et al., 1993; Tien Bui et al., 2015). Moreover, it has the advantages of a simple algorithm and preferable precision. Due to the existence of ISB, the traditional DGNSS model should set separate clock parameters for each system to ensure the precision of positioning results. As the introduction of the ISB can maximise the redundancy in multi-GNSS positioning, the performance of DGNSS is also expected to improve when ISB is introduced. However, previous research on ISB in a differential model is limited to systems such as GPS/GALILEO, which have an overlapping frequency. Moreover, the ISB applied in a differential model is estimated in advance, which will restrict real-time positioning applications because of unknown differential ISBs for a new receiver pair. Therefore, not only Galileo ISB but also the ISB of BDS and GLONASS are examined in our research. Furthermore, a real time DGNSS model accounting for ISB is proposed in this paper. This model is developed in accordance with the ISB characteristics of BDS/GLONASS/Galileo. Coordinate parameters are solved together with the ISB parameters without relying on external information. Compared to the traditional DGNSS model, the robustness of the model is enhanced after ISBs are initialised within several epochs. Moreover, the positioning performance is significantly improved in urban areas with few visible satellites.

In this contribution, we first present the method for evaluating the ISB for DGNSS positioning. Then, the data of zero or short baselines are collected using different sets of GNSS receivers. The characteristics of ISB for various receivers are analysed for four

satellite systems. Finally, the performance of DGNSS positioning accounting for the ISB is illustrated for the environment with limited satellite visibility in simulated and real scenarios.

2. METHOD OF EVALUATING THE ISB IN THE DGNSS MODEL. We mainly focus on differential GNSS that considers the ISB in four satellite systems. GPS/GALIEO/BDS are based on the code division multiple access, and GLONASS is based on Frequency Division Multiple Access (FDMA). Each GLONASS satellite transmits its signal on one of the twelve adjacent frequencies for one frequency band. Therefore, the ISBs among the four systems are complicated. In practical applications, single-frequency band observations are generally used for the DGNSS model. The ISB constituent becomes relatively simple because the multi-GNSS time bias has been eliminated in the DGNSS model.

DGNSS utilises a base station or a network of continuous operating reference stations with known positions and broadcast corrections between the pseudorange measurement and the computed geometric range. Real-time corrections based on the base station are applied to raw pseudorange observations collected by the roving receiver, which can cancel or reduce most error sources, such as the tropospheric and ionospheric errors, satellite orbital error and satellite clock error. The raw observational model of the base station is expressed as follows:

$$P_a^q = \rho_a^q + c \cdot (dT_a + B_a^{*(q)} + \tau^{*(q)}) - c \cdot (dt^q + b^q) + \alpha^q \cdot T_a + I^q + \varepsilon_a^q \tag{1}$$

where superscript q is a particular satellite, $^*(q)$ is the GNSS system to which a particular q satellite belongs, subscript a is the receiver; P is the raw pseudorange observation, ρ is the geometric range, c is the speed of light, dT is the receiver clock error, dt is the satellite clock error, B is the receiver code hardware delay, b is the satellite code hardware delay, α is the troposphere mapping function, T is the tropospheric delay, I is the ionospheric delay, ε is the code observation noise, and τ is the time bias between two systems. Note that $\tau = 0$ when $^*(q)$ is the reference system.

The difference between the computed geometry ρ and the raw pseudorange observation P is presented in Equation (2), where PRC_a^q is the pseudorange correction (PRC) computed by the base station.

$$PRC_a^q = c \cdot (dT_a + B_a^{*(q)} + \tau^{*(q)}) - c \cdot (dt^q + b^q) + \alpha^q \cdot T_a + I^q + \varepsilon_a^q \tag{2}$$

After correcting with the PRC, the tropospheric and ionospheric delays can be assumed to be completely removed for a short baseline. Therefore, the observational model of rover b can be expressed as:

$$P_b^q - PRC_a^q = \rho_b^q + c \cdot \bar{d}T^{*(q)} + \varepsilon_{ab}^q \tag{3}$$

where $\bar{d}T^{*(q)} = dT_b - dT_a + B_b^{*(q)} - B_a^{*(q)}$. Equation (3) is the traditional observational model for DGNSS.

In a traditional model, each system has a specific receiver clock parameter. However, if one system is selected as a reference system, the receiver clock of the other systems can be separated into two items. Suppose $^*(q)$ is the reference system. Then, the observational model of satellite i can be expressed as Equation (4). $B_{ab}^{*(qi)} = B_b^{*(i)} - B_a^{*(i)} - (B_b^{*(q)} - B_a^{*(q)})$,

https://doi.org/10.1017/S0373463316000825 Published online by Cambridge University Press

where i refers to a particular GPS/BDS/Galileo satellite, and $B_{ab}^{*(qi)}$ is zero when satellite i belongs to system $^*(q)$.

$$P_b^i - PRC_a^i = \rho_b^i + c \cdot (\bar{d}T^{*(q)} + B_{ab}^{*(qi)}) + \varepsilon_{ab}^i \tag{4}$$

As a consequence of the FDMA approach, different hardware biases exist in the GLONASS receiving channels even within one frequency band. In general, the receiving equipment of the same type experiences similar inter-channel biases, which can be removed to a large extent in the differential mode (Zinoviev, 2005). However, as more and more manufacturers have entered the GPS/GLONASS receiver market, GLONASS receivers from different manufacturers today show large differences in their inter-channel biases (Wanninger, 2012; Yamada et al., 2010). Therefore, Equation (5) similarly presents the observational formula of GLONASS for a rover segment, where r refers to a particular GLONASS satellite, and k denotes the channel number.

$$P_b^r - PRC_a^r = \rho_b^r + c \cdot (\bar{d}T^{*(q)} + B_{ab,k}^{*(qr)}) + \varepsilon_{ab}^r \tag{5}$$

$B_{ab}^{*(qi)}$ and $B_{ab,k}^{*(qr)}$ are the ISB terms for the new DGNSS model. As $B_{ab}^{*(qi)}$ refers to the ISB difference between two receivers, we call it the Differential ISB (DISB) (Odijk and Teunissen, 2013). Here, the DISB is the same as the ISB derived by the code Double Differenced (DD) observational model (Equation (6)) according to Odijk and Teunissen (2013) and Paziewski and Wielgosz (2014).

$$P_{ab}^{qi} = \rho_{ab}^{qi} + B_{ab}^{*(qi)} + \varepsilon_{ab}^{qi} \tag{6}$$

Therefore, the DISB can be applied in the DGNSS model (Equation (4)) if it is estimated by the DD model (Equation (6)) in advance. The DISB parameters in the DGNSS model can also be estimated with three coordinate parameters and one receiver clock parameter. If the DISBs are stable and estimated, positioning with four satellites in different systems can be realised in the succeeding epochs.

3. ANALYSIS OF DISB CHARACTERISTICS.

Based on the theory presented in Section 2, the DISB is related to the hardware of the two receivers. Therefore, the size of the DISB is closely related to the characteristics of the two receivers. The receiver pairs of same and different types are analysed in this section. To prove the stability and study the size of the DISB for mixed receiver pairs, results of the DISB estimation were analysed on the basis of real GNSS observational data from frequency band 1.

To obtain accurate DISB results, we determine the code DISB of the four systems based on the DD model (Odijk and Teunissen (2013) and Paziewski and Wielgosz (2014)) instead of Equations (4) and (5) in Section 2. The main reason is that the receiver clock of the reference system is eliminated in the DD model, and thus the computed DISB is less affected by other parameters. Moreover, all the experiments are based on the processing of zero or short baselines with station coordinates held fixed. As GPS is the most popular satellite system with strong reliability, it is selected as the reference system when the DISB is estimated. The time difference in the four systems in the broadcast navigation message is also considered, GPS time is used. Code DISB is estimated either in an 'instantaneous' (single-epoch) solution or in a multi-epoch (Kalman filter) solution.

https://doi.org/10.1017/S0373463316000825 Published online by Cambridge University Press

3.1. *DISB for receiver pairs of the same type.* The first experiment investigated the DISB for receiver pairs of the same type. The data were obtained from the campuses of Curtin University, which is gratefully acknowledged. Six receivers supporting the four GPS/GLONASS/GALILEO/BDS systems were connected to four TRIMBLE TRM 59800·00 antennae. Four short baselines formed by receiver pairs from the same manufactures were processed. Table 1 shows a general overview of the four receiver pairs, which include the receiver type, baseline length and observation session, among others. Note that the receiver pair CUTA-CUTC are of the same receiver type but are different versions. During the observation session, four Galileo satellites (E11, E12, E18 and E19) were available in the earlier session, and only one Galileo satellite (E11) was tracked in the latter. The number of satellites in the other three systems was greater than five in this period of time. One GLONASS DISB parameter was estimated because the receiver equipment of the same type had experienced similar inter-channel biases (Zinoviev, 2005; Yamada et al., 2010).

The single-epoch DISB results of the four baselines are illustrated in Figures 1 and 2 and Table 2. Particularly, the average and the standard deviation of the DISB for the three systems are calculated. Note that GPS is the reference system by default. The DISB of the BDS/GLONASS/Galileo systems is represented by blue, red and green, respectively. The Galileo DISB is close to zero in the receiver pairs (CUT3-CUBB, CUT2-CUTC and CUTB-CUTC) of the same receiver type and version. It should be noted that GPS and Galileo have an overlapping frequency on the L1 band. Therefore, the DISB can be ignored for two systems with an overlapping frequency together with the receiver pair of the same type and version. Similar conclusions were also derived from the work of Paziewski and Wielgosz (2014). However, in the case in which a baseline (CUTA-CUTC) forms with the same receiver type but with a different version, the estimated Galileo ISB amounts to −0·57 m, which is no longer close to zero. Moreover, the BDS DISB for the receiver pairs CUT2-CUTC and CUTB-CUTC amounts to −1·19 m and −0·36 m, respectively, although these two receiver pairs are of the same receiver type and version. This finding indicates that the Galileo DISB depends on the receiver type and version, but the BDS DISB may differ with individual receivers.

The standard deviations of the DISB are only a few decimetres, but the standard deviations of the Galileo readings are relatively higher at the end of the plots. During this period, as the number of Galileo satellites is only one, any bias in the data can easily be reflected in the estimated parameters when the elevation of the observed Galileo satellites is low. At

Table 1. General overview of the four receiver pairs.

Receiver pair		Baseline length	Remarks
JAVADTRE_G3TH_8 V3·6·2b2 (CUT3)	JAVADTRE_G3TH_8 V3·6·2b2(CUBB)	4·3 m	Observation session: 0:00–9:20, March 21, 2015 at Curtin Interval: 30 s Location: Curtin Constellation: GPS/GLONASS/ Galileo/BDS
TRIMBLE NETR9 V4·93 (CUT2)	TRIMBLE NETR9 V4·93 (CUTC)	7·1 m	
TRIMBLE NETR9 V4·85 (CUTA)	TRIMBLE NETR9 V4·93 (CUTC)	4·8 m	
TRIMBLE NETR9 V4·93 (CUTB)	TRIMBLE NETR9 V4·93 (CUTC)	6·2 m	

https://doi.org/10.1017/S0373463316000825 Published online by Cambridge University Press

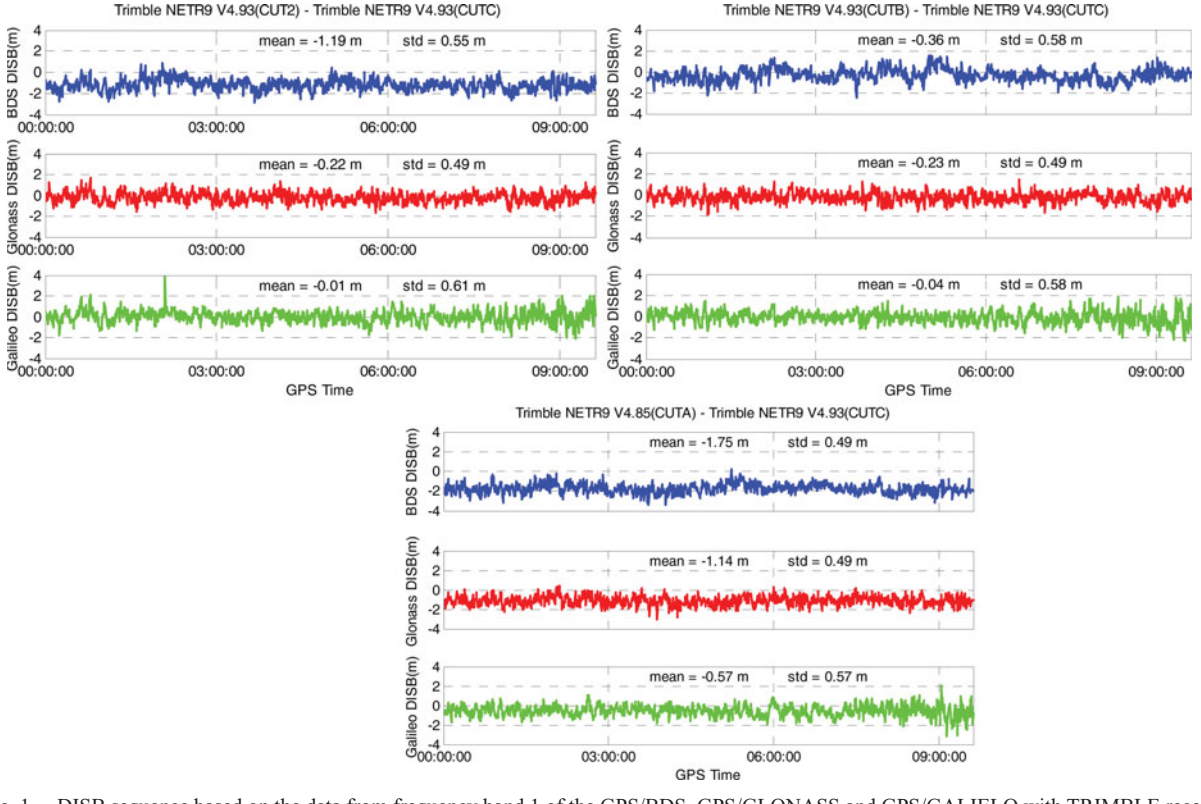

Figure 1. DISB sequence based on the data from frequency band 1 of the GPS/BDS, GPS/GLONASS and GPS/GALIELO with TRIMBLE receivers.

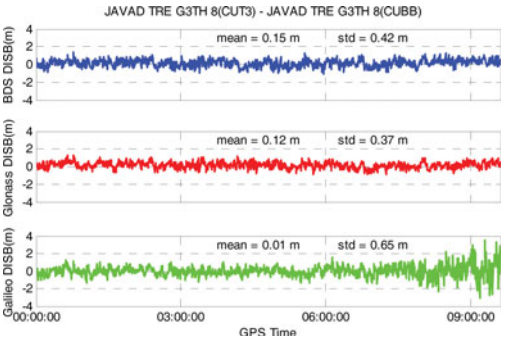

Figure 2. DISB sequence based on the data from frequency band 1 of the GPS/BDS, GPS/GLONASS and GPS/GALILEO with JAVAD receivers.

Table 2. Mean and standard deviation values of the DISB for receiver pairs of the same type.

	BDS (m)		GLONASS (m)		GALILEO (m)	
Receiver pair	mean	Standard deviation	mean	Standard deviation	mean	Standard deviation
CUT2-CUTC	−1·19	0·55	−0·22	0·49	−0·01	0·61
CUTB-CUTC	−0·36	0·58	−0·23	0·49	−0·04	0·58
CUTA-CUTC	−1·75	0·49	−1·14	0·49	−0·57	0·57
CUT3-CUBB	0·15	0·42	0·12	0·37	0·01	0·65

the same time, the standard deviations of the GLONASS DISB for the four baselines are smaller than those of the BDS and the Galileo and are almost distributed in white noise. This proves that the DISB difference among the 12 adjacent frequencies on the L1 band is not obvious for receiver pairs of the same type.

3.2. *DISB for receiver pairs of different types.* The data for this experiment were collected from Curtin University and Wuhan University. Three receivers of different types (SEPTENTRIO, TRIMBLE and JAVAD) called CUT1/CUT2/CUT3 were connected to the same antenna (TRM59800·00) using a signal splitter at Curtin. Three receivers from Chinese manufacturers (COMNAV, HI-TARGET and UNICORE) and a TRIMBLE receiver were also connected to an antenna at Wuhan. Table 3 is a general overview of five baselines formed by these receivers. To analyse the size and temporal stability of DISB, single-epoch and multi-epoch (20 epochs and 60 epochs, respectively) data were processed. Twelve GLONASS DISB parameters were estimated in this experiment because of the possible characteristic differences in the different receiver types.

Figure 3 presents the GLONASS DISB results of two receiver pairs (CUT1-CUT2 and CUT3-CUT2) associated with 12 channels. The DISB of different channels present apparent differences. The scopes of the GLONASS DISB for the SEPTENTRIO-TRIMBLE and JAVAD-TRIMBLE are (−3·15 m, −1·51 m) and (−0·26 m, 0·87 m), respectively. At the same time, the DISB of both receiver pairs present a significant linear relationship with the frequency channel number. In this case, the correlation coefficients of the two receiver pairs are −0·95 and −0·97. Additionally, the residuals of the least-squares fit for the two receiver pairs are 0·17 m and 0·09 m. The DISBs of the BDS and Galileo for these two receiver pairs are presented in Figure 4. In this case, the mean Galileo DISB value is 0·22 m and 0·17 m for the two receiver pairs, which means the hardware delay of the three receiver

https://doi.org/10.1017/S0373463316000825 Published online by Cambridge University Press

Table 3. General overview of the five receiver pairs.

Receiver pair		Constellations	Remarks
SEPTENTRIO (CUT1)	TRIMBLE (CUT2)	GPS GLONASS	Observation session: day 080, 2015 at Curtin Interval: 30 s Baseline length: 0·0 m
JAVAD (CUT3)	TRIMBLE (CUT2)	BDS GALILEO	
COMNAV (WHU2)	TRIMBLE (WHU1)		Observation session: day 330, 2015 at Wuhan Interval: 30 s Baseline length: 0·0 m
HI-TGAGET (WHU3)	TRIMBLE (WHU1)	GPS BDS	
UNICORE (WHU4)	TRIMBLE (WHU1)		

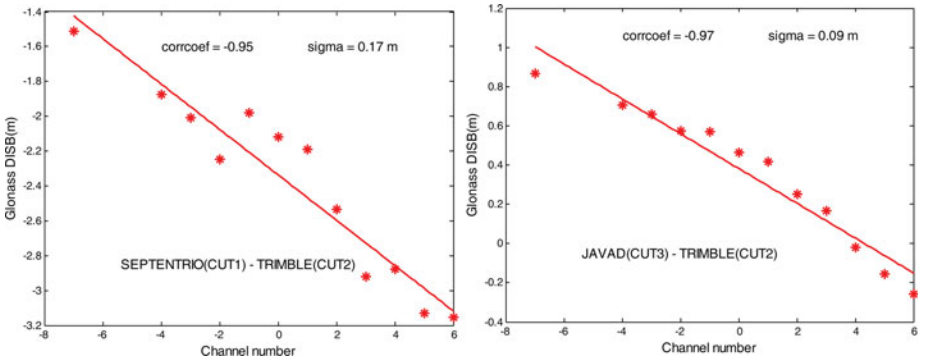

Figure 3. DISB results based on the data from frequency band 1 of GPS/GLONASS for receiver pairs of different types.

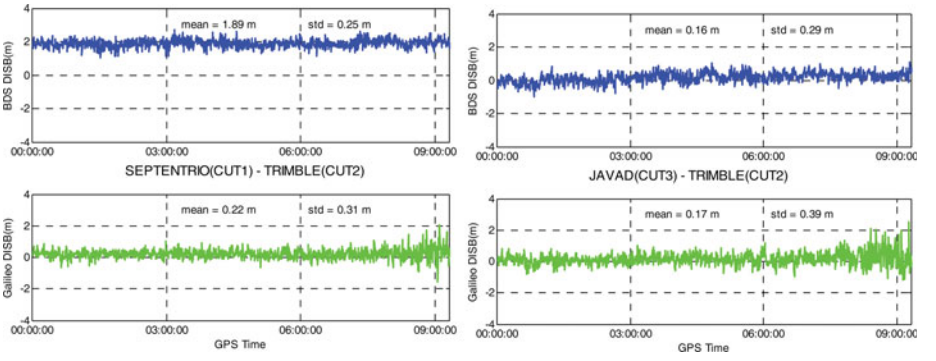

Figure 4. DISB results based on the data from frequency band 1 of GPS/BDS and GPS/Galileo between receiver pairs of different types.

https://doi.org/10.1017/S0373463316000825 Published online by Cambridge University Press

Table 4. Mean and standard deviation values of the BDS DISB for receiver pairs of different types.

	Mean (m)			Standard deviation (m)		
Receiver manufacturer	1 epoch	20 epochs	60 epochs	1 epoch	20 epochs	60 epochs
CUT1-CUT2	1·89	1·88	1·87	0·25	0·08	0·05
CUT3-CUT2	0·16	0·16	0·17	0·29	0·13	0·10
WUH2-WUH1	9·84	9·84	9·84	0·22	0·08	0·07
WUH3-WUH1	1·72	1·71	1·72	0·28	0·12	0·09
WUH4-WUH1	−8·11	−8·12	−8·12	0·34	0·14	0·11

types in these two receiver pairs show similar characteristics in the Galileo system. Note that the standard deviations of the DISB for these two receiver pairs are less than those of the receiver pairs in Section 3.1. The possible cause of this is that the multipath error has greatly reduced in the baseline connected to the same antenna.

Table 4 shows the repeatability of the BDS DISB estimated in the single-epoch solution and in the multi-epoch solution for the five baselines. The mean values of the BDS DISB estimation from the multi-epoch solution are in agreement with those of the single-epoch solution. The standard deviations of the single-epoch results for the five receiver pairs are also at the level of a few decimetres. The standard deviation of the DISB becomes smaller with increasing epochs. The precision of the DISB for some receiver pairs (SEPTENTRIO-TRIMBLE and COMNAV-TRIMBLE) can reach a few centimetres within 20 epochs. In this case, the sizes of the BDS DISB for COMNAV-TRIMBLE and UNICORE-TRIMBLE are 9·8 m and −8·1 m, respectively, which are statistically significant.

4. NEW COMBINED DGNSS MODEL AND POSITIONING RESULTS. According to the analysis in Section 3, the Galileo DISB can be ignored for receiver pairs of the same type and version. At the same time, the difference in the GLONASS DISB between adjacent frequencies can be neglected for receiver pairs of the same type. However, the size of BDS DISB varies with different receiver pairs even though the receiver pair is of the same type. Moreover, Galileo DISB is no longer close to zero for receiver pairs of different versions. As a result, estimating the DISB of various receiver pairs in advance and applying it to a new receiver pair when positioning with the DGNSS model is almost impossible. Fortunately, the several centimetre precision of the DISB can be obtained when estimated within tens of epochs by the Kalman filter. Therefore, the DISB can be estimated as constant parameters in real time for a new receiver pair. With respect to the GLONASS system, the DISB has an apparent linear relationship with the receiver pair JAVAD-TRIMBLE and SEPTENTRIO-TRIMBLE. In the study of Yamada et al. (2010), the code inter-channel bias of the L1 band also shows similar phenomena for the receiver pair NOVATEL-TRIMBLE, NOVATEL-JAVAD and NOVATEL-TOPCON. We propose using Equation (7) in DGNSS positioning including the GLONASS system for receiver pairs showing similar characteristics. In Equation (7), Δh is the difference between the two inter-channel biases for two receivers on adjacent GLONASS channels, k is the channel number and B^{GR}_{ab,k_0} is the DISB for channel number k_0.

$$P^r_b - PRC^r_a = \rho^r_b + \bar{d}T^G + B^{GR}_{ab,k_0} + (k^r - k_0) \cdot \Delta h + \varepsilon^r_{ab} \tag{7}$$

https://doi.org/10.1017/S0373463316000825 Published online by Cambridge University Press

The BDS/GLONASS/Galileo DISB parameters and one receiver clock parameter are estimated together with three coordinate parameters by the Kalman filter according to Equations (4) and (7). After the DISB is initialised for a few minutes, redundant information of the observational model increases and the performance of DGNSS positioning improves in a harsh environment such as urban canyons.

To verify the effect of the new combined DGNSS in a harsh environment, simulated data and the data collected in a real urban area were processed with the new and the traditional DGNSS model. The simulated data were obtained from the data collected from an open-sky environment handled in a particular condition. In this experiment, the data were from the receiver pair CUT1-CUT2 analysed in Section 3.2. To simulate the data collected in a disturbed circumstance, 2 + 2 + 2 + N satellites were selected by a random function during GPS time of 0:00:00–9:50:00. The cut-off elevation was set to 10°. 2 + 2 + 2 + N satellites referred to 2 GPS + 2 BDS + 2 GLONASS + all Galileo satellites available. Eight data sets were simulated by this receiver pair under the same restrictions. This simulated scenario could ensure DGNSS positioning with the traditional method (seven unknown parameters). Four DISB parameters (two for GLONASS) were estimated together with three coordinate parameters and one receiver clock parameter based on Equations (4) and (7).

Figure 5 shows one of the eight experiment results. Table 5 presents the average root mean square (rms) value of eight datasets for two models. Unlike in the traditional method, significant improvement is observed in both horizontal and vertical directions. In this case, the accuracy of east and north is improved by 61·6% and 60·9%, respectively, and the vertical accuracy is improved by 48·9%. At the end of the plots on the left of Figure 5, the precision of the traditional method is clearly degraded, and this damage is caused by the decreased number of Galileo satellites. During this period, the number of

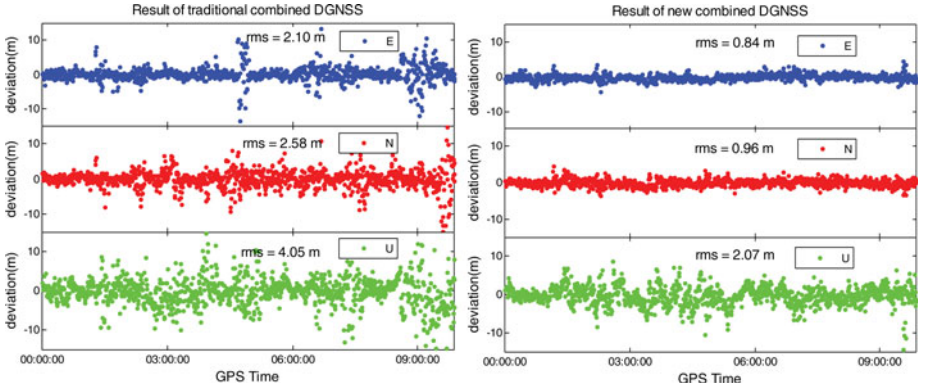

Figure 5. Comparison of the DGNSS positioning results between the traditional and new methods.

Table 5. Root mean square (rms) average value of the GNSS positioning results for eight simulations.

rms	Traditional model (m)	New model (m)	Improvement rate
East	2·11	0·81	61·6%
North	2·46	0·96	60·9%
Up	3·83	1·96	48·9%

https://doi.org/10.1017/S0373463316000825 Published online by Cambridge University Press

Galileo satellites is one until it disappears at 9:20:00. However, the precision of the new method does not decline because of the robustness enhanced after the DISBs are initialised. Another possible reason for lower accuracy positioning results in the traditional model is that GLONASS inter-channel bias is not considered.

To further analyse the benefits of the new combined model, dynamic data were also processed with the traditional and the new DGNSS model. The data were collected by two TRIMBLE receivers of different versions in the centre area of Xi'an where many buildings are located. The whole experiment lasted for about 2 h and 20 min from local time 11:20 to 13:40 on January 12, 2015. The sampling interval was 1 s and the cut-off elevation was set to 10°. Figure 6 shows the number of visible satellites during this time span, and the number changed greatly in the disturbed urban environment. To evaluate the precision of DGNSS positioning results, the results processed by NOVATEL SPAN served as reference (Soon et al., 2008). High-precision GNSS and inertial navigation can obtain reliable results even in troubled circumstances because of their integrating technology. Accuracy in the horizontal and vertical directions processed by the traditional and new combination models

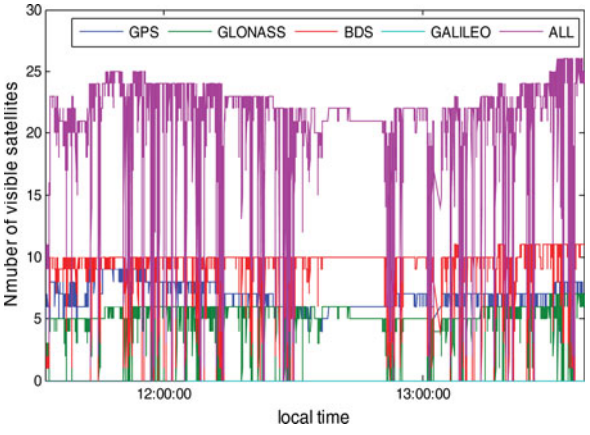

Figure 6. Number of visible satellites for four systems.

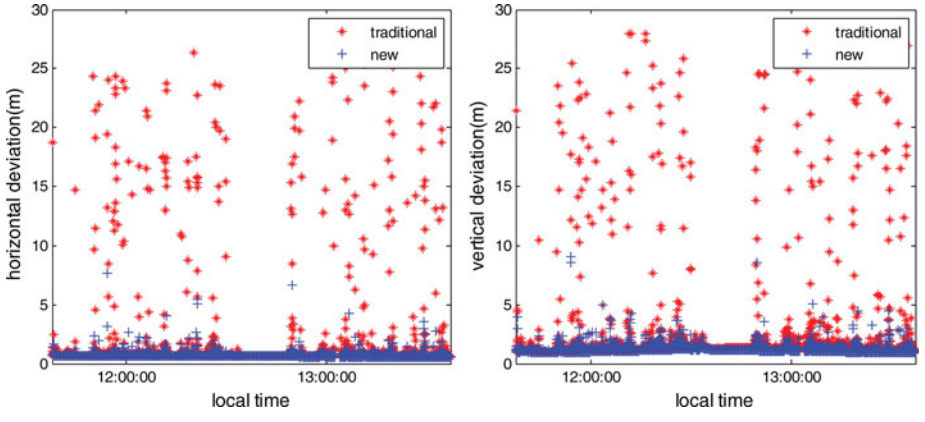

Figure 7. DGNSS positioning result in an urban environment.

https://doi.org/10.1017/S0373463316000825 Published online by Cambridge University Press

is presented in Figure 7. More positioning results are obtained by the new DGNSS model as positioning results can be obtained when the satellite number is more than 3 + N (N is the number of GNSS systems) of the traditional method. However, four satellites from arbitrarily the same or different systems are sufficient for the new model after the DISBs are initialised. Moreover, accuracy of the traditional method is greater than 5 m in both horizontal and vertical directions for some epochs. Aside from a few visible satellites, the multipath error and large noise in the observational signal are also the main causes. The observational error and the model error can easily damage the positioning results when redundant information is less. However, the positioning results of the new method are better because of the more redundant information after the DISBs are initialised within several epochs. Note that the precision of the new combined model does not improve when the satellite number is enough (e.g., more than 15), such as in the middle period of this experiment.

5. SUMMARY AND CONCLUSION. In this paper, we investigated the interoperability of DGNSS positioning with the current GPS/GLONASS/Galileo/BDS systems. In the traditional DGNSS observation model, four receiver clock parameters have to be resolved at the same time except for three coordinate parameters due to the clock difference between different systems. To obtain more reliable positioning results, the ISB is introduced in our research. Initially, it introduces additional parameters to be estimated. However, the ISBs in multi-systems related to the new DGNSS model are stable for a particular receiver pair according to our research. The DISB difference in the adjacent frequencies on the L1 band of GLONASS can be neglected for a receiver pair of the same type. Moreover, the DISB of Galileo-GPS can be ignored for a receiver pair of the same type and version. In view of the DISB characteristics of multi-GNSS, we propose that DISB can be estimated as constant parameters in real time by the Kalman filter when the rover coordinate parameters are solved by the DGNSS model. The precision of the DISB can reach 2–3 decimetres in a single-epoch solution and several centimetres in tens of epochs. As a result, the DGNSS observational model is strengthened by maximising the redundancy information after the DISBs are initialised. Based on the numerical computation results, the horizontal and vertical precision of the new model has obviously improved in a complex circumstance with poor geometry satellites compared with the traditional DGNSS model.

ACKNOWLEDGMENTS

This work is funded by the National Key Research and Development Program of China (No. 2016YFB0800405). In addition, it is a part of the project “Research on the Perception Technology about the Essential Factor of Chang Jiang Waterway and its Application” (No. 2013-364-548-200), which is supported by the Chang Jiang Waterway Bureau. This work is also a part of the project “Construction of Network RTK Management Software Platform for Continuous Reference Station” (2016-070-204-020-158). All this support is gratefully acknowledged. The authors are grateful to anonymous reviewers for their insightful comments, which have helped to improve the quality of the paper.

REFERENCES

Ashkenazi, V., Hill, C.J., Ochieng, W.Y. and Nagle, J. (1993). Wide-Area Differential GPS: A Performance Study. *Navigation*, **40**(3), 297–319.

Cai, C. and Gao, Y. (2009). A Combined GPS/GLONASS Navigation Algorithm for use with Limited Satellite Visibility. *Journal of Navigation*, **62**(4), 671–685.

Dalla Torre, A. and Caporali, A. (2015). An analysis of intersystem biases for multi-GNSS positioning. *GPS Solutions*, **19**(2), 297–307.

Deng, C., Tang, W., Liu, J. and Shi, C. (2014). Reliable single-epoch ambiguity resolution for short baselines using combined GPS/BeiDou system. *GPS Solutions*, **18**(3), 375–386.

He, H., Li, J., Yang, Y., Xu, J., Guo, H. and Wang, A. (2014). Performance assessment of single-and dual-frequency BeiDou/GPS single-epoch kinematic positioning. *GPS Solutions*, **18**(3), 393–403.

Kremer, G.T., Kalafus, R.M., Loomis, P.V. and Reynolds, J.C. (1990). The effect of selective availability on differential GPS corrections. *Navigation*, **37**(1), 39–52.

Montenbruck, O., Hauschild, A. and Hessels, U. (2011). Characterization of GPS/GIOVE Sensor Stations in the CONGO Network. *GPS Solutions*, **15**(3), 193–205.

Odolinski, R., Teunissen, P.J.G. and Odijk, D. (2014). Combined BDS, Galileo, QZSS and GPS single-frequency RTK. *GPS Solutions*, **19**(1), 151–163.

Odijk, D. and Teunissen, P.J.G. (2013). Characterization of between-receiver GPS-Galileo inter-system biases and their effect on mixed ambiguity resolution. *GPS Solutions*, **17**(4), 521–533.

Paziewski, J. and Wielgosz, P. (2014). Accounting for Galileo-GPS inter-system biases in precise satellite positioning. *Journal of Geodesy*, **89**(1), 81–93.

Shi, C., Zhao, Q., Hu, Z. and Liu, J. (2013). Precise relative positioning using real tracking data from COMPASS GEO and IGSO satellites. *GPS Solutions*, **17**(1), 103–119.

Schaer, S. (1999). Mapping and predicting the Earth's ionosphere using the Global Positioning System. *Geod.-Geophys. Arb. Schweiz*, **59**, 59.

Sardón, E. and Zarraoa, N. (1997). Estimation of total electron content using GPS data: How stable are the differential satellite and receiver instrumental biases? *Radio Science*, **32**(5), 1899–1910.

Soon, B.K., Scheding, S., Lee, H.K., Lee, H.K. and Durrant-Whyte, H. (2008). An approach to aid INS using time-differenced GPS carrier phase (TDCP) measurements. *GPS Solutions*, **12**(4), 261–271.

Tien Bui, D., Tran, C.T., Pradhan, B., Revhaug, I. and Seidu, R. (2015). iGeoTrans–a novel iOS application for GPS positioning in geosciences. Geocarto International, **30**(2), 202–217.

Wanninger, L. (2012). Carrier-phase inter-frequency biases of GLONASS receivers. *Journal of Geodesy*, **86**(2), 139–148.

Yamada, H., Takasu, T., Kubo, N. and Yasuda, A. (2010, September). Evaluation and calibration of receiver inter-channel biases for RTK-GPS/GLONASS. *Proceedings of ION GNSS*, 1580–1587.

Zhang, W., Cannon, M.E., Julien, O. and Alves, P. (2003). Investigation of combined GPS/GALILEO cascading ambiguity resolution schemes. *Proceedings of ION GPS/GNSS*, 2599–2610.

Zinoviev, A.E. (2005). Using GLONASS in combined GNSS receivers: current status. *Proceedings of ION GNSS*, 1046–1057.